

# Segmental patterning of the vertebrate embryonic axis

Mary-Lee Dequéant\* and Olivier Pourquié\*\*†

**Abstract** | The body axis of vertebrates is composed of a serial repetition of similar anatomical modules that are called segments or metameres. This particular mode of organization is especially conspicuous at the level of the periodic arrangement of vertebrae in the spine. The segmental pattern is established during embryogenesis when the somites — the embryonic segments of vertebrates — are rhythmically produced from the paraxial mesoderm. This process involves the segmentation clock, which is a travelling oscillator that interacts with a maturation wave called the wavefront to produce the periodic series of somites. Here, we review our current understanding of the segmentation process in vertebrates.

## Somites

Embryonic segments (epithelial blocks of tissue surrounding a cavity called somitocoel) giving rise to the sclerotome (precursors of the axial skeleton) and dermomyotome (precursors of the dermis of the back and skeletal muscles).

## Presomitic mesoderm

A mesoderm-derived mesenchymal tissue lying on both sides of the neural tube that gives rise to the somites.

## Paraxial mesoderm

A mesodermal tissue comprising the head mesoderm and the somitic mesoderm.

## Otic vesicle

One of the paired sacs of invaginated ectoderm that develops into the inner ear.

\**Stowers Institute for Medical Research* and †*Howard Hughes Medical Institute, 1000 East 50<sup>th</sup> Street, Kansas City, Missouri 64110, USA.*  
Correspondence to O.P.  
e-mail:

[olp@stowers-institute.org](mailto:olp@stowers-institute.org)  
doi:10.1038/nrg2320

Published online  
15 April 2008

Vertebrate somites are epithelial blocks of mesoderm containing the precursors of the vertebrae and the skeletal muscles (FIG. 1). They form rhythmically from the presomitic mesoderm (PSM) at a time period that is characteristic of the species, ranging from 30 minutes in zebrafish embryos, 90 minutes in chicken and 120 minutes in mouse, to approximately 4–5 hours in humans<sup>1</sup>. Pairs of somites regularly pinch off synchronously from the anterior tip of the PSM in an anterior-to-posterior sequence until a defined number, also characteristic of the species, is reached. Although this number is usually highly constrained within a given species, it varies widely between species, ranging from approximately 30 pairs of somites in some fish to several hundred in snakes<sup>2</sup>. The somitic lineage is part of the paraxial mesoderm in amniote species such as chicken, mouse and human, and is part of the dorsal mesoderm in lower vertebrates such as fish and frog. In all vertebrates, the somitic series begins anteriorly immediately caudal to the otic vesicle (FIG. 1) and runs posteriorly on both sides of the neural tube and notochord to the caudal tip of the embryo. The first five somites are incorporated into the basi-occipital bone at the base of the skull, whereas the more posterior somites form the vertebral column<sup>3</sup>.

Somitogenesis in amniotes can be subdivided into three main phases (FIG. 1). First, during the specification phase, the descendants of the epiblast and later on of the tail bud acquire a paraxial mesoderm identity. These cells are progressively added to the posterior tip of the embryo to form the PSM. During the second phase, a segmental pre-pattern manifests as a stripe of gene expression that is established in the anterior PSM.

This pre-pattern provides the blueprint from which the morphological segment — the somite — will be formed during the final phase. Then, the rostrocaudal polarity of the future somite is established in the newly specified segment. This rostrocaudal subdivision of somites controls the segmentation of the nervous system by restricting migration of neural crest cells and axons to the anterior part of the somites<sup>4</sup>. This subdivision is also responsible for the definitive patterning of vertebrae that form when the posterior part of one somite fuses to the anterior part of the consecutive somite during a process called resegmentation. Finally, the formation of the morphological boundaries results in the separation of the epithelial somite from the PSM<sup>5</sup>. Soon after their formation, somites subdivide into the ventral sclerotome that contains the precursors of the axial skeleton and the dorsal dermomyotome that contributes to the myotome and dermatome, which form the skeletal muscles and dermis of the back, respectively<sup>6</sup>. Finally, depending on their position along the anteroposterior (AP) axis, somite derivatives acquire a defined anatomical identity that is imposed mainly by Hox genes that control their subsequent regional differentiation<sup>7,8</sup>. The mechanisms underlying the rostrocaudal subdivision and maturation of the somites have been reviewed<sup>6,9–11</sup> and will not be discussed here further. Instead, we focus on the mechanisms involved in the generation of the metamer in the PSM, an aspect of somitogenesis that has received the most attention over the past 10 years since the identification of an oscillator associated with this process called the segmentation clock.

**The segmentation clock oscillator**

During the past three decades, the fly embryo has been the major paradigm for the study of segmentation. The pioneering screens for segmentation defects in *Drosophila melanogaster* led to a thorough understanding of the molecular cascade controlling the establishment of the segmental pattern in this organism<sup>12,13</sup>. The process is initiated by gradients of maternal gene products, such as *bicoid* and *nanos*, which then activate a series of zygotic gap genes such as *hunchback* and *Kruppel*, the expression domains of which are sequentially organized in broad stripes along the AP axis of the embryo. The combinatorial expression of the gap genes then results in the periodic expression of the pair-rule genes, which include *hairy*, *even-skipped* and *runt*, in seven alternating domains that pre-figure the 14 embryonic segments. The combinatorial expression of the pair-rule genes, in turn, activates the segment polarity genes (such as *engrailed*, *wingless* and *hedgehog*) that establish the definitive segmental pattern of the embryo.

However, in contrast to the fly, most other segmented species add segments sequentially as the embryonic axis progressively elongates posteriorly (FIG. 1). Such a rhythmic mode of segment formation is observed in vertebrates. It inspired theoretical models such as the ‘clock and wavefront’ model<sup>14</sup>, which proposed that PSM cells forming a somite undergo an abrupt change in cellular properties that could be formalized by a particular type of mathematical catastrophe (FIG. 2a). Such a catastrophe can be explained by a bistable transition between two steady states, allowing an abrupt switch from one particular state to another<sup>15</sup>. To account for the periodic occurrence of the catastrophe, the existence of an oscillator that controls the response of PSM cells to the mechanism triggering the catastrophe was postulated (FIG. 2a). A number of subsequent models were proposed, many of which also relied upon the conversion of a temporal oscillation into a spatial periodic pattern<sup>16,17</sup>.

The first evidence of the existence of an oscillator coupled to somitogenesis was provided by the periodic expression of the mRNA encoding the transcription factor HES1 (hairy and enhancer of split 1) in the chicken embryo PSM<sup>18</sup>. During the formation of each somite, the PSM is swiped by a dynamic wave of HES1 mRNA expression (FIG. 2b). These transcriptional oscillations of HES1 that occur with the same periodicity as the somitogenesis process were proposed to identify a molecular oscillator — termed the segmentation clock — acting in PSM cells. Subsequently, several other genes exhibiting such a cyclic behaviour were identified in fish, frog and mouse, indicating that the oscillator is conserved in vertebrates<sup>19–22</sup>. These genes are now referred to as cyclic genes and, as we shall see below, the vast majority of them belong to the Notch, Wnt and fibroblast growth factor (FGF) signalling pathways. Much of the recent research in the vertebrate segmentation field has focused on the identification of the pacemaker that triggers the rhythmic expression of the cyclic genes in the PSM. This has led to several hypotheses that are discussed in this Review.

**The zebrafish oscillator**

In zebrafish, all the cyclic genes identified so far belong to the Notch pathway and comprise the Notch downstream targets: *her1* (hairy and enhancer of split-related 1), *her7*, *her11*, *her12* and *her15* (which are homologous to the chicken HES1)<sup>19,23–28</sup>, as well as the Notch ligand *DeltaC*<sup>21</sup>. Large genetic screens carried out in zebrafish have identified a handful of mutants in which somitogenesis is disrupted<sup>29</sup>. These mutants show alterations

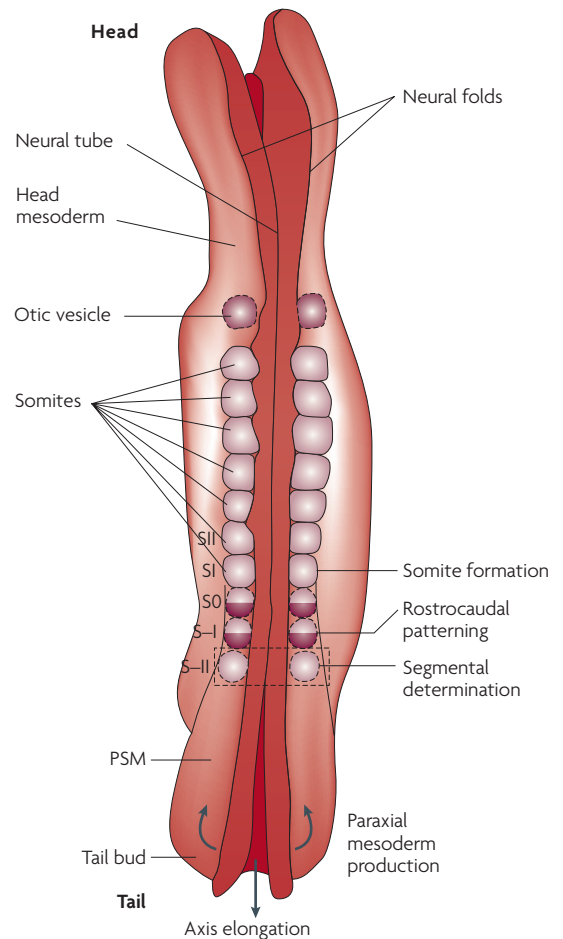


**Figure 1 | Establishment of segmentation during embryogenesis.** Dorsal view of a 4-week-old human embryo showing somites and the presomitic mesoderm (PSM) forming the paraxial mesoderm that flanks the axial neural tube. The different phases of paraxial mesoderm patterning leading to somite formation are indicated as: paraxial mesoderm production from the progenitor pool localized in the tail bud, segmental determination, rostro-caudal patterning and somite formation. The anterior-most somites give rise to the basi-occipital bone of the skull and to the anterior-most cervical vertebrae. The subsequent somites generate the vertebral column. Prospective somites in the PSM are numbered in a rostrocaudal series beginning with somite S0, which is the forming somite, in negative roman numerals (for example, –I, –II)<sup>132</sup>. The segmented somites (for example, S-I, S-II) are numbered according to Ordahl<sup>133</sup>. Arrows indicate the movement of paraxial mesoderm cells from the tail bud into the PSM.

**Amniotes**

Group of tetrapod vertebrates including mammals, reptiles and birds, the embryo of which is protected by a membrane called the amnion, in particular from dehydration.

**Epiblast**

Tissue precursor of the three germ layers during gastrulation.

**Metamery**

A segmented organization of the body plan along the anterior–posterior axis.

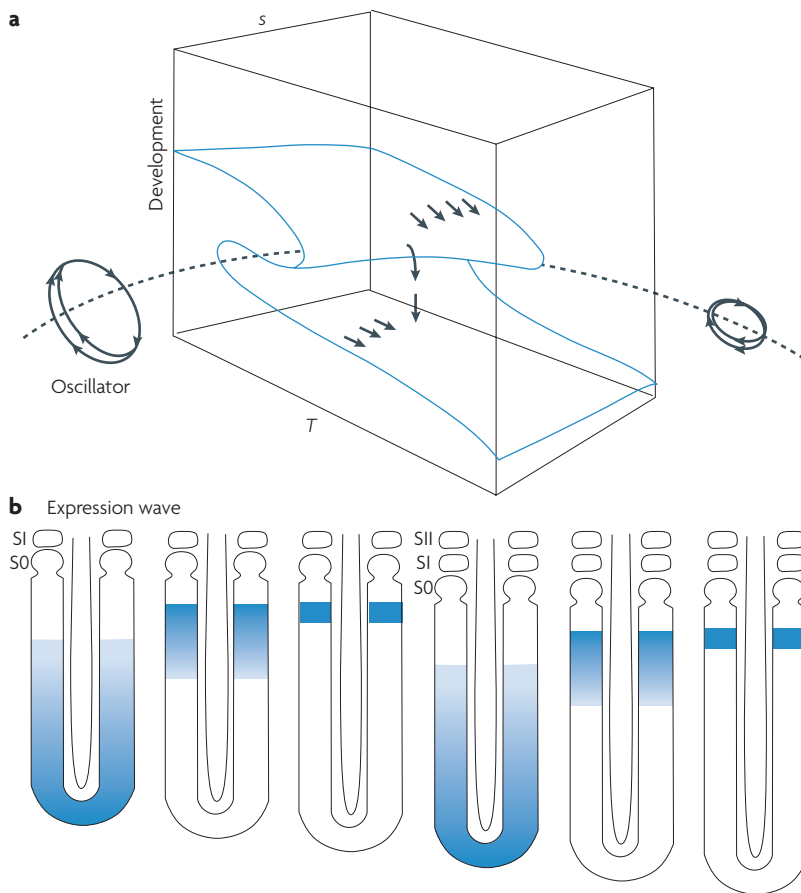


**Figure 2 | The clock and wavefront model and the segmentation clock oscillator.** **a** | Topological representation of the somitogenesis model showing a section of the embryonic axis (corresponding to the posterior part of the embryo, including the presomitic mesoderm (PSM) and the few somites most recently formed) plotted in real space (*s*) (in head–tail axis), real developmental time (*T*) (that is, indicating the onset of each somitic cycle) and a dimension representing intracellular development (the vertical arrows falling from the fold-edge symbolize the catastrophe and correspond to abrupt cellular changes associated with somite formation). The oscillator (circle) was postulated to ensure the periodic occurrence of the catastrophe (in the fold-edge, along the dashed line) that corresponds to an abrupt transition between two cellular states. **b** | Evidence for an oscillator underlying vertebrate segmentation. Periodic waves of transcriptional expression of the *hairy1* gene (blue) in PSM cells are associated with the formation of each pair of somites added sequentially<sup>18</sup>. Part **a** modified with permission from REF. 14 © (1976) Elsevier Ltd.

in genes that encode components of the Notch pathway, such as the *Notch1A* receptor, the ligands *DeltaD* and *DeltaC*, and the *Mindbomb* ubiquitin ligase that is required for Delta endocytosis and Notch activation<sup>19,30–32</sup>. In these mutants, the dynamic wave of cyclic gene expression in the PSM is disrupted and replaced by a salt-and-pepper expression pattern<sup>21</sup>. This characteristic expression pattern of the cyclic genes in the Notch mutants was proposed to reflect desynchronized oscillations in PSM cells<sup>21</sup>, suggesting a role for Notch signalling in the synchronization of the oscillations among PSM cells (BOX 1).

Experiments in zebrafish embryos in which the function of the Her genes was blocked by mutation or by morpholino knock-down, or constitutively activated

by overexpression<sup>19,24,25,30,33–37</sup> led to a simple oscillator model that essentially relied on the Her1 and Her7 transcriptional repressors. In this model, oscillations are generated by a negative feedback loop in which the Her genes are directly repressed by their own protein products<sup>36</sup> (BOX 1). To generate oscillations, the model takes into account a defined time delay in the auto-inhibitory circuit that occurs from the beginning of transcription of the Her RNA until the Her protein binds to the Her gene promoter. Mathematical modelling showed that oscillations can be sustained, but only if the half-lives of the gene transcripts and proteins are short compared with the sum of the transcriptional and translational delays<sup>36</sup>. Using plausible numerical values for the model parameters, oscillations exhibiting a period consistent with that observed in zebrafish could be obtained<sup>36</sup>. Several of the kinetic parameters (such as transcriptional delays and the stability of the RNAs and proteins) that were initially roughly estimated, were subsequently validated in the embryo and shown to be consistent with the estimated values<sup>35</sup>. Surprisingly, whereas a complete disruption of segmentation would be expected in zebrafish mutant embryos lacking both *her1* and *her7*, or in embryos injected with *her1* and *her7* morpholinos, these embryos still form abnormal somites<sup>25</sup>. However, redundancy with the other Her genes could account for this surprisingly mild phenotype.

This Her1–Her7 intracellular oscillator was proposed to be linked to an intercellular oscillator involving the Notch signalling pathway. Her1 and Her7 negatively regulate *deltaC*, thus potentially triggering oscillations of this Notch ligand (BOX 1) that should, in turn, result in periodic Notch activation in neighbouring cells<sup>24,31</sup>. This coupling provides a basis for maintaining the synchrony between oscillations of neighbouring cells<sup>21</sup> (BOX 1).

It remains unclear whether the Notch pathway is required for Her oscillations. The fact that the first oscillatory cycles require Her genes but not the Notch pathway<sup>38</sup> argues that Notch is not part of the clock pacemaker. Accordingly, Her gene expression is not abolished in the Notch pathway mutants or when treating embryos with the  $\gamma$ -secretase inhibitor DAPT (*N*-[*N*-(3,5-difluorophenacetyl)-*L*-alanyl]-*S*-phenyl glycine *t*-butyl ester)<sup>19,24,38</sup>. However, a constitutively active form of Notch1A results in overexpression of *her1* in the PSM<sup>33</sup>, suggesting that these genes are targets of the Notch pathway. This is also consistent with the observation that in many biological systems, genes of the Her family of transcription factors function as downstream targets of Notch<sup>39</sup>. Furthermore, it has been proposed that the Notch ligand *DeltaD* is required for the initiation of oscillations in the tail bud<sup>40</sup>.

The Her1–Her7 oscillations require the *Hes6*-related gene, *Her13.2* (REF. 41). Expression of this transcription factor is regulated by FGF signalling. It can form a heterodimer with Her1, enhancing the ability of Her1 to negatively regulate its own promoter<sup>41</sup> (BOX 1). Thus, although in fish the Her1–Her7 negative feedback loop might constitute the core of the segmentation clock pacemaker, it requires additional input from several signalling pathways<sup>42</sup>.

**Morpholinos**  
Synthetic molecules of antisense oligonucleotides used for gene expression knock-down.

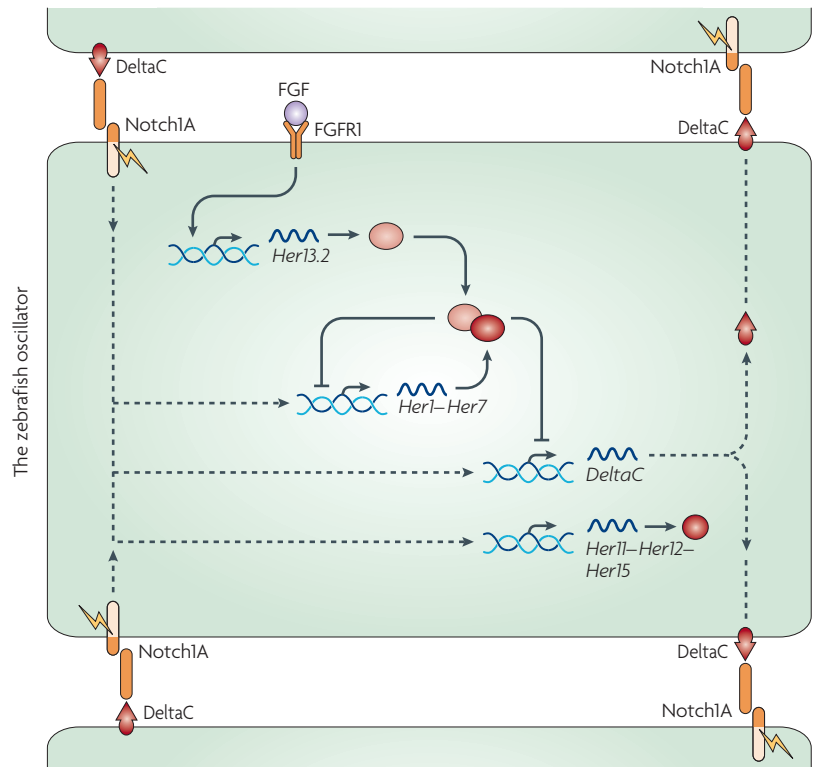
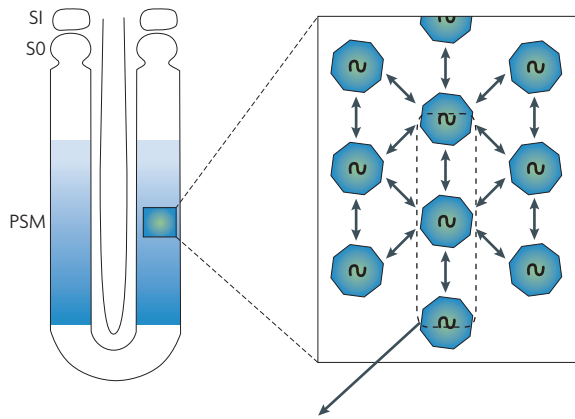
Box 1 | Synchronization of the presomitic mesoderm (PSM) cellular oscillators

A remarkable property among neighbouring PSM cells is their synchronized oscillations, resulting in the smooth transcriptional wave that sweeps through the PSM (cyclic gene expression is shown in blue in PSM cells that are represented as octagons). In zebrafish, the role of the Notch pathway in synchronizing oscillators was first proposed based on the typical salt-and-pepper expression pattern of cyclic genes in PSM cells of Notch segmentation mutants<sup>19,21</sup>, interpreted as desynchronized oscillations<sup>21</sup>. In these mutants in which the first somites segment normally, oscillations would be set initially, but owing to the lack of Notch-dependent coupling, they would progressively drift out of synchrony, resulting in segmentation failure<sup>21,38</sup>.

The role of the Notch pathway in coupling oscillators has been mathematically modelled by connecting the zebrafish *Her1* (hairy and enhancer of split-related 1)–*Her7* intracellular oscillator to the Notch–DeltaC (DeltaC is a Notch ligand) intercellular loop<sup>35,36,130</sup>. The transcription factors *Her1* and *Her7* establish a negative feedback loop that is proposed to function as the zebrafish clock pacemaker and to control the periodic repression of *DeltaC*, allowing the synchronous activation of Notch signalling in neighbouring cells. In addition to receiving inputs from Notch signalling, the *Her1*–*Her7* oscillator requires the *Her13.2* partner, which is downstream of FGF (fibroblast growth factor) signalling.

Experimental evidence supports the role of cell–cell communication through the Notch–DeltaC loop in maintaining synchronized oscillations among nearby cells. Implantation of cells from a zebrafish embryo overexpressing *DeltaC* can desynchronize the waves of cyclic gene expression, resulting in the shifting of somitic boundaries on the injected side<sup>128,129</sup>. Consistently, dissociation of the PSM cells rapidly results in a loss of synchronized oscillations in chicken<sup>130</sup> and mouse<sup>131</sup>. The coupling between cellular oscillators provided by the Notch–Delta intercellular loop is thought to confer robustness to the synchronized clock oscillations<sup>38</sup> (E. Ozbudak and J. Lewis, personal communication) against developmental noise such as cell proliferation, cell movement or stochastic gene expression.

FGFR1, FGF receptor 1.



**The amniote oscillator**

The first cyclic genes identified in amniotes also belong to the Notch pathway<sup>18</sup>. As in zebrafish, oscillations of the hairy and enhancer of split (called *Hes* in amniotes) homologues are detected in chicken (*HES1*, *HAIRY2* and *HEY2*) and in mouse (*Hes1*, *Hes7*, *Hes5* and *Hey1*)<sup>18,43–46</sup>. Oscillations of the Notch ligand-encoding *Dll1* (delta-like 1) have also been reported in mouse<sup>47</sup>. Cyclic expression of other Notch pathway genes such as *Lfng* (lunatic fringe), which is a glycosyl-transferase that modifies the Notch receptor, is detected only in amniotes<sup>20,48,49</sup> and not in lower vertebrates<sup>50</sup>. As the first cyclic genes identified in amniotes were targets of the Notch pathway, the first molecular models placed Notch signalling as a central component of the segmentation clock<sup>51,52</sup>. This idea was supported by the

observation that *Lfng* and *Hes1* expression was lost in the PSM of mouse Notch pathway mutants such as *Rbpjk* (recombination signal binding protein for immunoglobulin kappa J region) and *Dll1* homozygotes<sup>43,53</sup>. Furthermore, periodic expression in the mouse PSM of the cleaved activated intracytoplasmic form of the Notch1 receptor is detected by immunohistochemistry, providing direct evidence for rhythmic activation of the pathway<sup>54,55</sup>. In the chicken embryo, *LFNG* is periodically activated by Notch signalling in the PSM and, in turn, inhibits Notch signalling, thereby establishing a negative feedback loop<sup>56</sup> (FIG. 3). The expression of the *LFNG* protein cycles with the same period as somitogenesis in the PSM, indicating a short half-life<sup>56</sup>. In mouse *Lfng*-null mutants, constitutive expression of the activated form of Notch is detected in the PSM,

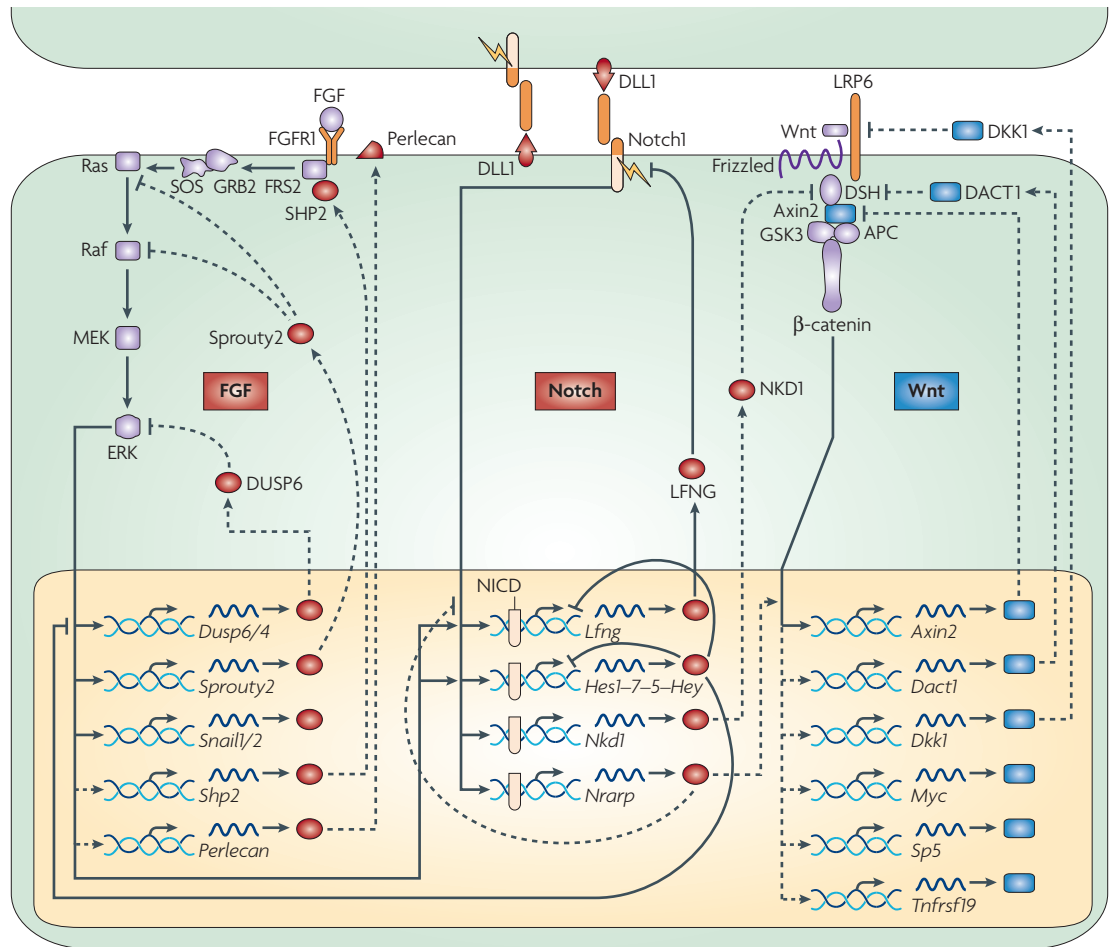


**Figure 3 | The mouse oscillator.** Cyclic genes belonging to the Notch and FGF (fibroblast growth factor) pathways (the products of which are indicated in red) oscillate in opposite phase to cyclic genes of the Wnt pathway (blue). A large number of the cyclic genes are involved in negative feedback loops. The basic circuitry of the three signalling pathways is represented. Dashed lines correspond to modes of regulation inferred from work in other systems or based on microarray data<sup>70</sup>. APC, adenomatous polyposis coli; DACT1, dapper homologue 1; DKK1, dickkopf homologue 1; DLL1, delta-like 1; DSH, dishevelled; DUSP6, dual specificity phosphatase 6; ERK, mitogen-activated protein kinase 1; FGFR1, FGF receptor 1; GRB2, growth factor receptor-bound protein 2; GSK3, glycogen synthase kinase 3; *Hes1*, hairy and enhancer of split-related 1; LFNG, lunatic fringe; LRP6, low density lipoprotein receptor-related protein 6; MEK, mitogen-activated protein kinase 1; NICD, Notch intracellular domain; NKD1, naked cuticle 1 homologue; *Nrarp*, Notch-regulated ankyrin repeat protein; SHP2, Src homology region 2-containing protein tyrosine phosphatase 2; SOS, son of sevenless; *Sp5*, trans-acting transcription factor 5; *Tnfrsf19*, tumour necrosis factor receptor superfamily, member 19.

supporting a conserved role for this negative feedback loop in amniote segmentation<sup>55</sup> (FIG. 3). However, constitutive overexpression of *Lfng* in the PSM of transgenic mice does not prevent oscillations of the endogenous *Lfng* or *Hes7* (REF. 57), suggesting that this negative feedback loop is, by itself, insufficient to drive the oscillatory network.

In mouse, the HES protein family has a key role in the control of oscillations by implementing a negative feedback loop similar to the zebrafish Her-based loop<sup>58</sup>. The genes *Hes7*, *Hes1*, *Hes5* and *Hey2* encode transcriptional repressors that are expressed periodically in the mouse PSM<sup>43–46</sup>. The *Hes1*, *Hes5* and *Hey2*-null mutants do not show any somitic phenotype, but in *Hes7*-null mutants somitogenesis is defective and oscillations of cyclic genes such as *Lfng* are disrupted<sup>59–62</sup>. Furthermore,

transcription of both *Hes7* and *Lfng* is upregulated in the *Hes7* mutants, consistent with the idea that *Hes7* represses its own transcription in the PSM as well as that of *Lfng*<sup>58</sup> (FIG. 3). Analysis of the regulatory region of the *Lfng* promoter confirmed that it includes CSL (CBF1, Su(H), LAG1) binding sites that are required for regulation by Notch signalling<sup>63</sup>, as well as binding sites for bHLH (basic helix-loop-helix) proteins, such as members of the Hes family<sup>64</sup>. Deletion of these regulatory sites (clock elements) blocks *Lfng* oscillations in the posterior PSM<sup>65</sup>. This leads to a ubiquitous activation of Notch in the PSM and to severe vertebral anomalies. Strikingly, however, this phenotype is not observed in the sacral (posterior-most region of the trunk) and caudal (tail) region, suggesting that the clock regulation might vary along the AP body axis.

Mathematical models, based on a delayed negative feedback loop that is controlled by Hes-family members similar to those proposed to drive fish cyclic gene oscillations, have been proposed for the mouse embryo<sup>66,67</sup>. In these models, the production of oscillations directly depends on the half-life of the Her/Hes RNA and protein. The rapid clearing of the cyclic genes from the PSM is consistent with a short half-life of the mRNA of the cyclic genes. The mouse HES7 and HES1 proteins also have a short half-life that is actively controlled by the proteasome and estimated to be approximately 22 minutes *in vitro*<sup>58,66,68</sup>. To test the importance of protein stability in the generation of oscillations, the half-life of HES7 was genetically modified in the mouse embryo. A point mutation conferring a small half-life increase from 22 to 30 minutes leads to a failure of *Hes7* oscillations and somite segmentation, as predicted by the time-delay model<sup>66</sup>.

Unlike in zebrafish, several other signalling pathways show periodic activity in the mouse PSM during the segmentation clock cycle. Identification in mouse of oscillations of *Axin2*, a key negative feedback inhibitor of the Wnt pathway, together with the observation that in mice with the hypomorphic *Wnt3a* mutation vestigial tail (*vt*) both *Axin2* and *Lfng* oscillations are disrupted, suggested the implication of Wnt signalling in the oscillator mechanism<sup>69</sup>. A microarray-based approach led to the identification of a much larger number of cyclic genes that are associated with the segmentation clock in the mouse PSM transcriptome<sup>70</sup> (FIG. 3). The cyclic genes that were identified fell into two main clusters of gene expression profiles that oscillate in antiphase (FIG. 3). One cluster contained a large number of cyclic genes, most of which are linked to the Wnt signalling pathway (shown in blue in FIG. 3). These cyclic genes correspond to downstream targets of the Wnt pathway such as the transcription factors *SP5* (trans-acting transcription factor 5)<sup>71</sup> and *MYC* (myelocytomatosis oncogene)<sup>70,72</sup>. These also include negative feedback inhibitors such as *AXIN2* (REF. 69) and *DKK1* (dickkopf homologue 1)<sup>73</sup>. Although *Axin2*<sup>-/-</sup> mutants do not exhibit any somitic phenotype<sup>74</sup>, inactivation of many of the newly identified cyclic genes in the Wnt cluster (*Dkk1* (REF. 75), *Sp5* (REF. 76), *Myc* (REF. 77) and *has2* (hyaluronan synthase 2)<sup>78</sup>) produces segmentation defects, supporting a role for Wnt signalling during segmentation in mouse.

Wnt activation in cells results in stabilization of  $\beta$ -catenin, which in turn enters the nucleus to activate the expression of target genes. Therefore, oscillations of Wnt inhibitors such as *DKK1* or *DACT1* (dapper homologue 1) should, in principle, result in the rhythmic fluctuation of  $\beta$ -catenin expression levels. As Wnt signalling has been shown to function upstream of both Wnt and Notch oscillations<sup>69</sup>, such  $\beta$ -catenin oscillations seem to be a good candidate for a pacemaker that entrains the Notch signalling loop. Accordingly, Notch and Wnt cyclic gene oscillations are lost in a conditional deletion of  $\beta$ -catenin in the PSM<sup>79</sup>. However, in a mouse mutant in which  $\beta$ -catenin is made constitutively stable in the PSM, expression of Wnt and Notch pathway genes still oscillates<sup>79,80</sup>, indicating that  $\beta$ -catenin signalling is necessary but insufficient for driving the expression of

cyclic genes. Therefore, these experiments argue against a role for the periodic destabilization of  $\beta$ -catenin in the control of clock oscillations.

The second cyclic gene cluster that was identified in the microarray study<sup>70</sup> contains known cyclic genes of the Notch pathway as well as other genes of this pathway that had not been previously associated with the oscillator (FIG. 3). These include *Nrarp* (Notch-regulated ankyrin repeat protein), which is a direct target of Notch signalling that functions as a negative regulator of the Notch pathway<sup>81–83</sup>. In parallel, NRARP can also positively regulate the Wnt pathway by stabilizing the transcription factor *LEF1* (lymphoid enhancer binding factor 1)<sup>84</sup>. The previously identified cyclic gene naked cuticle 1 homologue (*Nkd1*), an inhibitor of Wnt signalling regulated by Notch signalling<sup>85</sup>, was also identified as part of the Notch cluster (FIG. 3). These genes might provide a functional link between the Notch and Wnt arms of the oscillator.

A novel class of cyclic genes involved in FGF signalling and oscillating in phase with the Notch cyclic genes was identified in the same microarray study<sup>70</sup>. Two negative feedback inhibitors of the FGF pathway, *Spry2* (sprouty homologue 2) and *Dusp6* (dual specificity phosphatase 6), show a clearly periodic profile in the array series (FIG. 3). The FGF targets *Snail1* (snail homologue 1), in mouse, and *SNAIL2*, in chicken<sup>86</sup>, as well as the *Dusp4* negative feedback inhibitors of the FGF pathway<sup>87</sup>, also exhibit periodic expression in mouse and chicken PSM. Furthermore, periodic phosphorylation of *ERK* (extracellular signal-regulated kinase) in the mouse PSM supports periodic FGF signalling activity<sup>87</sup>.

Despite the synchronized activation of Notch and FGF activity in the clock cycle, expression of FGF-regulated genes seems to be largely independent of Notch signalling as *Spry2* expression is still dynamic in *Rbpjk*<sup>-/-</sup> mutant mice<sup>70</sup>. Furthermore, *Dusp4* expression is still cyclic in *Lfng*<sup>-/-</sup>, *Dll1*<sup>-/-</sup> and *Rbpjk*<sup>-/-</sup> mutants as well as in mouse PSM treated with DAPT<sup>87</sup>. However, conditional deletion of *Fgfr1* (FGF receptor 1) in the PSM blocks the oscillations of the FGF, Notch and Wnt pathways in the PSM<sup>87,88</sup>. Moreover, whereas treatment of mouse tail explants with the FGFR1 inhibitor SU5402 quickly abolishes cyclic expression of *Axin2* and *Spry2*, it only blocks *Lfng* oscillations after a one-cycle delay, indicating that FGF indirectly regulates the Notch oscillations<sup>88</sup>. The requirement of Wnt signalling for *Lfng* oscillations<sup>89,90</sup> suggests that FGF functions upstream of Wnt signalling, which, in turn, controls Notch oscillations. In mouse, the Notch target *Hes7* also requires FGF signalling<sup>87</sup>. FGF was proposed to be required to initiate *Hes7* pulses of expression in the tail bud, whereas propagation of *Hes7* oscillations in the more anterior PSM requires Notch signalling<sup>87</sup>. Such a two-step model is consistent with the observed delay of *Lfng* oscillation inhibition when FGFR1 is inhibited. However, *Lfng* stripes are observed in the PSM of a mouse conditional *Fgfr1*<sup>-/-</sup> mutant with a constitutively stable form of  $\beta$ -catenin<sup>80</sup>. Therefore, constitutive  $\beta$ -catenin restores Notch oscillations in the absence of FGF signalling, arguing against a role for FGF as the periodic input controlling Wnt

oscillations. Therefore, these experiments argue that neither periodic Wnt nor FGF signalling triggers the rhythmic expression of cyclic genes such as *Lfng*. Together with observations indicating that *Axin2* oscillations are maintained in Notch pathway mutants<sup>69</sup>, this suggests that none of the three oscillating pathways of the segmentation clock functions as a pacemaker. Therefore, it cannot be ruled out that these oscillatory networks of signalling genes correspond only to outputs of an as yet unidentified pacemaker. On the other hand, the evolutionary conservation of the role of the Her/Hes proteins is consistent with their potential role in the pacemaker of the segmentation clock.

A striking feature of the cyclic gene network in amniotes is its apparent redundancy. Among mouse cyclic genes are several negative feedback inhibitors for each of the Notch, FGF and Wnt pathways (FIG. 3) that potentially account for the robustness of the network. Other cyclic genes are likely to be just downstream targets of the clock and could merely represent outputs of the oscillator. The role of the segmentation clock might be to deliver coordinated pulses of Notch, FGF and Wnt signalling that are, in turn, used for the appropriate patterning of the segments. Below we discuss how this periodic signalling is translated into a coordinated striped gene activation that defines the segmental domain and its boundaries.

#### Translating the clock pulse into segments

In the original clock and wavefront model, Cooke and Zeeman postulated the existence of a front of maturation — the wavefront — that slowly moves posteriorly along the embryo<sup>14</sup>. When PSM cells in the permissive phase of the clock oscillation cycle are passed by the wavefront, they undergo an abrupt transition (a catastrophe) that leads to somite formation (FIG. 2a). Therefore, the wavefront serves to translate the rhythmic pulse of the clock into the spatial periodic series of segments. In the Cooke and Zeeman model, the wavefront was positioned at the anterior-most level of the PSM where somites form. This positioning was subsequently challenged by heat-shock experiments in *Xenopus*<sup>91</sup> that identified and positioned the hidden wavefront of cellular change more posteriorly than initially proposed. In chicken embryos, microsurgical inversions of small fragments of the PSM along the AP axis demonstrated the existence of a virtual boundary — called the determination front — in this tissue<sup>92</sup>. This boundary separates the posterior PSM domain (where inverted blocks of cells form segments according to their new position) from an anterior domain (where cells are committed to their original segmental fate). Therefore, the determination front was defined as the level at which PSM cells first acquire their segmental identity, and is therefore conceptually similar to the wavefront. At the molecular level, the position of the determination front corresponds to the posterior boundary of the *Mesp2* (mesoderm posterior 2) stripe that marks the first evidence of a segmental prepatterning in the PSM.

Interestingly, this transition in the PSM also corresponds to a morphological transition at the cellular level. Whereas the posterior PSM is a loose mesenchyme,

the cells located anterior to the determination front become progressively epithelialized. This transition is also accompanied by a slowing down of PSM cell movements<sup>93</sup>. The mesenchymal–epithelial transition that occurs concomitantly with the segmental patterning of the anterior PSM correlates with a downregulation of the *Snai* genes that are regulated by FGF signalling and are associated with a mesenchymal state in many systems<sup>86</sup>. Downregulation of *Snai* genes at the determination front correlates with the expression of several adhesion molecules such as integrins and cadherins, which progressively increases in the anterior PSM as cells become polarized<sup>94–96</sup>. This transition is also accompanied by the deposition of a basal lamina, containing laminin and fibronectin, that surrounds the anterior PSM<sup>95</sup>. This epithelialization process requires the bHLH transcription factor *TCF15* (transcription factor 15, also known as *Paraxis*) that is expressed anteriorly to the determination front in the anterior PSM and somites<sup>97</sup>. *TCF15* controls the activity of Rho GTPases, such as *RAC1* (Ras-related C3 botulinum substrate 1) and *CDC42* (cell division cycle 42 homologue), which have been shown to mediate the mesenchymal–epithelial transition during somite formation<sup>98</sup>.

The position of the determination front is defined by specific thresholds of FGF and Wnt signalling activities<sup>69,92,99</sup> (FIG. 4). The FGF gradient was first described as a posterior-to-anterior gradient of *Egf8* mRNA in the PSM of chicken, fish and mouse embryos<sup>92,99,100</sup>. This mRNA gradient is subsequently translated into a protein gradient and then into a MAPK (mitogen-activated protein kinase)–AKT activity gradient along the PSM<sup>93,99,100</sup>. The role of the FGF signalling gradient in positioning the determination front was first demonstrated by experiments that perturbed the slope of the gradient in chicken embryos. This was achieved by grafting FGF8-soaked beads next to the PSM or by overexpressing an *FGF8*-expressing construct in the PSM by electroporation<sup>92</sup>. This resulted in an anterior extension of posterior PSM markers, such as *Brachyury*, and in downregulation of segmentation and differentiation markers such as *paraxis*, *Mesp2* and *Myod* (myogenic differentiation 1)<sup>92,93</sup>.

*Egf8* loss-of-function mutations have proved to be more problematic to interpret owing to redundancy in the FGF pathway. Neither the zebrafish *fgf8* mutant *ace*<sup>101</sup> nor the conditional deletion of *Fgf8* in the mouse PSM<sup>102</sup> shows a segmentation phenotype, suggesting that FGF8 is not the only ligand involved in setting the FGF-signalling gradient along the PSM gradient. *Fgf3*, *Fgf4* and *Fgf18* are expressed in the PSM and tail bud region of the mouse embryo<sup>88</sup>. In zebrafish, *fgf8* functions redundantly with *fgf24* to promote the formation of the posterior PSM<sup>103</sup>. Inhibition of FGF signalling was achieved by treating chicken embryos with pharmacological inhibitors<sup>92</sup>. This resulted in a posterior shift of the anterior boundary of the expression domain of genes such as *FGF8* that are associated with a posterior identity. Such a posterior shift was also observed for the expression domain of posterior markers *Fgf8* and *Msgn1* (mesogenin 1) in mouse mutant embryos

#### Mesenchyme

Tissue consisting of loosely packed cells.

#### Basal lamina

A layer of extracellular matrix that underlies the epithelium and is secreted by the epithelial cells.

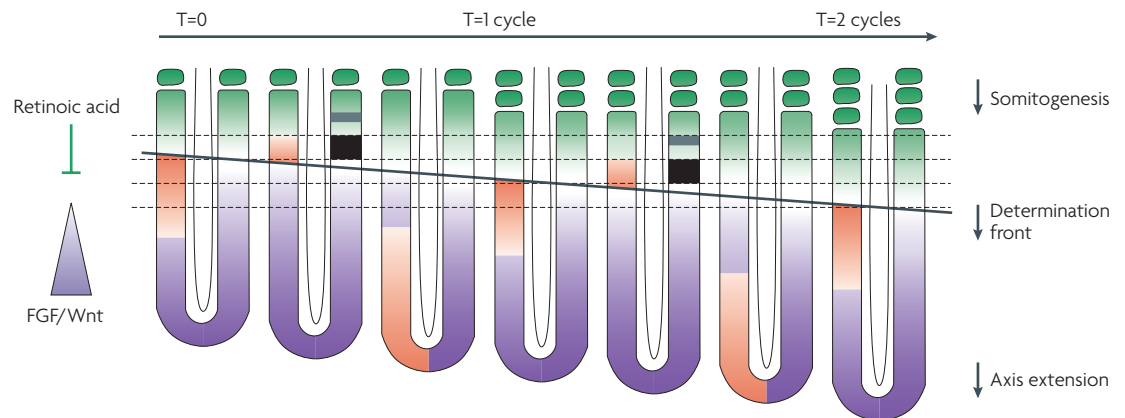


**Figure 4 | A somitogenesis model integrating the segmentation clock and determination front.** The system of opposing gradients of FGF (fibroblast growth factor)–Wnt signalling (purple) and retinoic acid (green) signalling was proposed to position the determination front (black line) along the presomitic mesoderm (PSM). This particular level is characterized by a signalling threshold at which the cells become competent to respond to the segmentation clock signal and is conceptually similar to the wavefront of the original Cooke and Zeeman model<sup>14</sup>. The clock signal is still poorly characterized but probably involves three signalling pathways experiencing periodic activity: FGF, Wnt and Notch. The wave of cyclic gene expression controlled by the segmentation clock oscillator is shown in orange on the left side of the embryos. When competent cells that pass through the determination front receive the clock signal, they simultaneously activate *Mesp2* (mesoderm posterior 2; shown in black), thereby defining the future segmental domain as shown on the right side of the embryos. In this model, the size of the segment (the future somite) is defined by the distance travelled by the wavefront during one oscillation of the segmentation clock. However, the role of retinoic acid in this model remains debated (see text). During the next cycle *Mesp2* expression becomes restricted to the anterior compartment of S–I (grey). T, time in segmentation clock cycle unit.

with a conditional deletion in the paraxial mesoderm of FGFR1, the only FGF receptor that is expressed in the PSM<sup>88</sup>. Together, these data suggest that high levels of FGF signalling are required to maintain the posterior identity of PSM cells<sup>92</sup>. This further led to the idea that the progressive decrease in FGF signalling activity along the PSM defines a specific threshold below which the cells become competent to respond to the signalling pulse that is delivered by the segmentation clock (FIG. 4). The position of this threshold was proposed to correspond to the determination front<sup>92</sup>.

Wnt genes, such as *Wnt3a*, are expressed in the tail bud and posterior PSM<sup>69</sup>. Furthermore, a gradient of nuclear  $\beta$ -catenin extends from the tail bud to the determination front<sup>80</sup>. Together with the graded expression of Wnt targets, such as *Axin2*, along the PSM, they identify a posterior-to-anterior Wnt signalling gradient in the PSM parallel to the FGF gradient<sup>69</sup>. *Fgf8* expression is absent in *Wnt3a* mutants, indicating that Wnt signalling is required for the expression of FGF ligands in the PSM<sup>69</sup>. However, only a partial FGF gain of function is observed in the PSM of mouse embryos overexpressing a constitutively stable  $\beta$ -catenin, suggesting that Wnt signalling is insufficient for *Fgf8* expression in the PSM<sup>80</sup>. The posterior  $\beta$ -catenin gradient was recently shown to define the size of the oscillatory field in the PSM, thereby controlling the position of the wavefront where the oscillations stop<sup>80</sup>. Furthermore,  $\beta$ -catenin gain of function in the PSM prevents activation of MESP2 targets, indicating that downregulation of Wnt signalling at the determination front is required for normal segmentation to proceed<sup>79,80</sup>.

Whereas both FGF and Wnt signalling are characterized by posterior-to-anterior gradients of activity in the posterior PSM, some of their targets exhibit an oscillatory expression, which seems paradoxical. The  $\beta$ -catenin gain-of-function experiments demonstrate a role for the nuclear  $\beta$ -catenin gradient in the control of the maturation of cells along the PSM, but they indicate that oscillation of Wnt targets, such as *Axin2*, results from an oscillating input that is independent of  $\beta$ -catenin and FGF signalling<sup>80</sup>. Such an input could be provided by a pacemaker that is external to the cyclic gene network. Although similar gain-of-function experiments remain to be carried out for FGF signalling, such a pacemaker could also function on the FGF cyclic genes and explain the coexistence of a graded signal and an oscillatory response.

Retinoic acid (RA)<sup>104–107</sup> was also proposed to have a role in positioning the determination front as an anterior-to-posterior gradient of RA opposing the Wnt–FGF gradient<sup>108,109</sup> (FIG. 4). *RALDH2*, the RA biosynthetic enzyme, is expressed in the anterior-most PSM and segmented region, and is excluded from the tail bud and posterior PSM<sup>110</sup>. Using a RARE (RA response element)–LacZ reporter mouse, RA signalling was found to be restricted to the anterior PSM and segmented region, and absent from the posterior PSM and tail bud<sup>104</sup> where *CYP26*, an enzyme of the cytochrome P450 family that is involved in RA degradation, is expressed downstream of FGF<sup>111</sup>. In chicken, treatment of posterior PSM explants with RA agonists can downregulate *FGF8* expression, and a graft of an FGF8-soaked bead in the PSM represses *RALDH2* expression in the embryo<sup>108</sup>. Furthermore, in *Raldh2*



mouse mutants and in chicken or quail embryos that are deprived of RA, the *Fgf8* expression domain is extended along the PSM<sup>105,108</sup>. A similar antagonistic action of FGF and RA gradients was also observed in *Xenopus*, suggesting that this gradient system is conserved among vertebrates<sup>109</sup>. These experiments led to a proposal that the mutual inhibition of the FGF and RA gradients has a role in positioning the determination front. However, this is difficult to reconcile with the observation that somites do form in the *Raldh2* mouse mutant in which no RA signalling is detected<sup>112</sup>, suggesting that RA signalling is dispensable for somite formation. Furthermore, in the *Fgfr1* conditional knock-out, no significant posterior shift of the RARE-lacZ domain is observed, suggesting that FGF is not the only antagonist of the RA gradient<sup>88</sup>. Whether the posterior Wnt gradient, by itself, can antagonize RA signalling remains to be investigated.

RA has also been implicated in the control of the symmetry of the somitogenesis process<sup>104–107</sup>. Somite formation is asymmetric in embryos that are deprived of RA. This lateralized desynchronization of somitogenesis occurs in response to the activation of the left–right machinery that is involved in the asymmetric positioning of the internal organs. RA prevents the paraxial mesoderm from responding to the asymmetric signal downstream of *Nodal*, thereby maintaining the symmetry of the somitogenesis process at early stages.

In the embryo, the segmentation process is tightly coordinated with axis elongation through the formation of the FGF signalling gradient in the posterior PSM<sup>113</sup>. As the embryo grows posteriorly owing to axis elongation, new cells enter the posterior PSM, compensating for the loss of the anterior PSM cells that form somites. Transcription of the *Fgf8* mRNA is restricted to the PSM precursors in the tail bud, and it ceases when their descendants enter the posterior PSM. Therefore, as the axis elongates, cells become located progressively more anteriorly in the PSM and their *Fgf8* mRNA content progressively decays. This results in the establishment of an *Fgf8* mRNA gradient that is converted into a graded distribution of ligand and FGF activity<sup>93,99,113</sup>. A similar mechanism is assumed to be responsible for establishing the Wnt gradient<sup>89</sup>. As a result of the progressive decay of FGF–Wnt family mRNA and proteins in PSM cells, the determination front is constantly displaced posteriorly, and the speed of this displacement defines the speed that somitogenesis progresses along the AP axis (FIG. 4). This mechanism ensures a tight coordination between axis elongation and segmentation during embryogenesis.

#### A clock and wavefront-based model

Experimental perturbations of the shape of the FGF, Wnt and RA gradients led to specific somite defects that revealed how the clock and the wavefront could interact. In zebrafish and chicken embryos, FGF- and Wnt-bead graft experiments shift the determination front anteriorly and lead to the formation of smaller somites<sup>69,92,99</sup>. Similarly, RA loss of function in mouse *Raldh2* mutants or in RA-deprived chicken or quail embryos results in an FGF gain of function in the PSM, leading to the same phenotype<sup>104,105,108</sup>. Conversely, inhibition of FGF

signalling shifts the determination front posteriorly, resulting in the formation of larger somites<sup>92,99</sup>. Conditional deletion of *Fgfr1* in the PSM also results in transient formation of larger somites followed by disruption of segmentation<sup>88</sup>.

These results gave rise to a new segmentation model integrating the original clock and wavefront concepts<sup>14</sup>. In this model, the wavefront corresponds to the travelling determination front, defined as a threshold of Wnt–FGF–RA signalling, the position of which moves posteriorly and accompanies the posterior regression of these gradients. During one segmentation clock oscillation, the determination front moves posteriorly along the AP axis by a distance that corresponds to approximately one somite (FIG. 4). We proposed that when PSM cells are passed by the determination front, they become competent to respond to a periodic signal delivered by the segmentation clock<sup>92</sup>. In response to this signal, the cohort of cells located between the determination front and the posterior boundary of the segment that was determined in the previous segmentation cycle simultaneously activate *Mesp2*, resulting in the formation of a stripe of *Mesp2* expression that prefigures the future segment. Once expressed, *Mesp2* stabilizes *Lfng* expression in the newly formed striped domain, leading to an inhibition of Notch signalling in this territory<sup>55</sup>. Because Notch is activated in the posterior part of the segmental domain that is located immediately anterior to the *Mesp2–Lfng* domain<sup>114</sup>, this mechanism generates an interface between cells activating and repressing Notch<sup>55</sup>. This interface marks the level of the future somite boundary. During the next oscillation cycle, the newly specified segmental domain becomes located more anteriorly in the PSM by one somite. Cells in this territory begin to activate a complex genetic programme downstream of MESP2. These cells activate the transcriptional repressor *Ripply1* that establishes a negative feedback loop shutting down *Mesp2* expression in the future posterior compartment<sup>115,116</sup>. MESP2 also activates the expression of genes, such as *Epha4* (Eph receptor A4), that are involved in boundary formation<sup>117</sup>. This complex genetic cascade ultimately results in the specification of the anterior and posterior somite compartments and of the somite boundaries.

A striking feature of the segmental patterning process is the highly synchronized periodic gene activation that occurs in the stripes of cells that define the future segments. The signalling pulse that is delivered by the segmentation clock is a good candidate to trigger this periodic gene activation. The synchronization of the response to this signal in the future segment was proposed to reflect a molecular switch that simultaneously triggers *Mesp2* expression in the cohort of competent cells that passed the determination front<sup>15</sup>. Mathematical modelling shows that the mutual inhibition of FGF and RA signalling can define a bistability domain along the PSM in which such a switch behaviour can be observed<sup>15</sup> (FIG. 5). In response to an appropriate signal, cells located in the bistability domain (in fact, in the area between the determination front and the last specified segment) can abruptly switch from the FGF-dominated steady

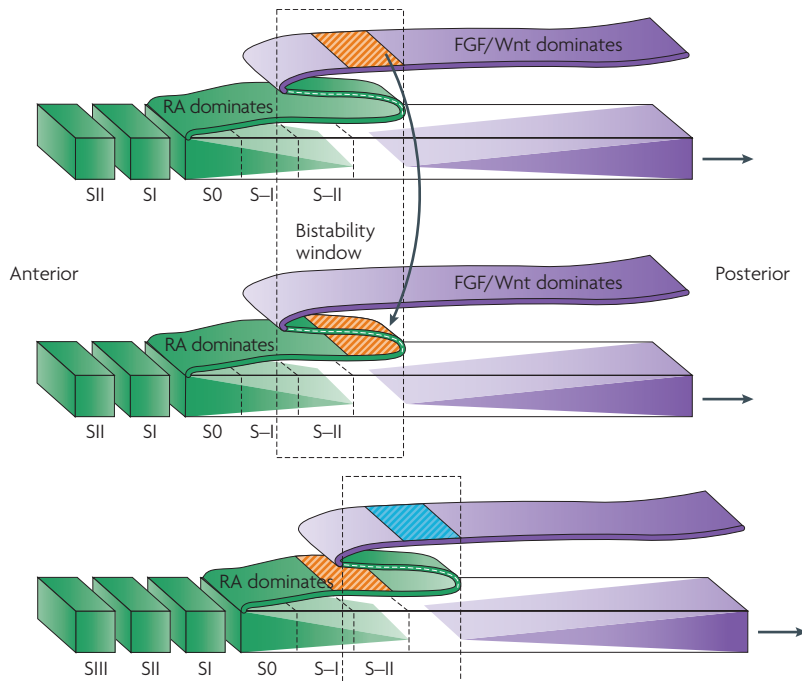


**Figure 5 | Model for segment determination.** The system of opposing FGF (fibroblast growth factor)–Wnt (purple) and retinoic acid (RA) (green) gradients was proposed to define a bistability window (dashed rectangle) in which cells can adopt either of two distinct steady states (FGF-dominated or RA-dominated<sup>15</sup>). In the bistability window, upon suprathreshold stimulation, cells that are in the FGF-dominated state can abruptly switch to the RA-dominated steady state, resulting in the simultaneous exposure of a cohort of cells (the future segment, in hatched orange) to RA signalling. This stimulation was proposed to be provided by the periodic signalling pulse delivered by the segmentation clock. Owing to the posterior extension of the axis and the decay of the FGF–Wnt mRNA and ligands in the PSM, the bistability window constantly moves posteriorly. The next cohort of cells to be simultaneously determined to form the future segment is hatched in blue. In this model, the posterior edge of the bistability window (bifurcation point) corresponds to the determination front.

**Suprathreshold stimulation**

Stimulation of sufficient strength to produce a perceptible effect; in the current context a catastrophe leading to somite determination.

**Urbilateria**

Hypothetical last common ancestor of all bilaterians.

**Bilateria**

Members of the animal kingdom that have bilateral symmetry — the property of having two similar sides, with definite upper and lower surfaces, and anterior and posterior ends.

**Ultradian oscillator**

Oscillator with a period of less than 24 hours.

state to the other, RA-dominated steady state<sup>15</sup> (FIG. 5). The signalling pulse that is generated by the segmentation clock is a good candidate to trigger the switch-like transition. This transition would result in a synchronous exposure of cells of the future segmental domain to RA signalling, thereby explaining the collective gene activation in the stripe of cells. This hypothesis is consistent with the observation that *Mesp2* and thylacine expression is repressed by FGF and controlled by Notch and RA signalling<sup>93,109,114</sup>. Remarkably, a similar bistable behaviour working together with an autonomous clock is observed in *in silico* simulations of segmentation controlled by a moving gradient, as in the clock and wavefront model<sup>118</sup>.

**Conclusion**

Studies of the segmentation clock oscillator in vertebrates have begun to shed light on the complex mechanism that is involved in generating the characteristic periodic pattern of the vertebrate body axis. A common strategy, based on an oscillator (the segmentation clock) that generates a temporal periodicity and a travelling maturation front that converts the signalling pulse into

a spatial periodic pattern, was identified in fish, frog, chicken and mouse embryos, supporting some conservation of the segmentation mechanism among vertebrates. A metameric pattern similar to that of vertebrates is also found in many invertebrate phyla such as arthropods and annelids<sup>119</sup>. Some arthropods in which axis formation and segmentation proceeds sequentially as in vertebrates, such as spiders, do show dynamic expression of Notch pathway genes during segment formation, suggesting that a molecular oscillator could operate in these species<sup>120</sup>. However, a very different segmentation machinery lacking cyclic genes has been identified in *D. melanogaster*. Furthermore, other invertebrates (including molluscs, nematodes and urochordates) are not segmented, raising the question of the conservation of segmentation in evolution<sup>119</sup>. So, it still remains unclear whether segmentation appeared independently in different phyla during evolution or whether it represents an ancestral feature of urbilateria, the ancestor of bilaterian animals.

Other examples of periodic structures generated by an oscillator include the well-characterized circadian pattern of sporulation in *Neurospora crassa*, which results in the formation of stripes of spores that are deposited daily in the rice tubes<sup>121</sup>. In plants, many structures, such as shoots and roots, are produced by progressive growth from a terminal growth zone (the meristem). This mechanism resembles that involved in producing the vertebrate AP body axis. Shoots and roots are often subdivided into repeated units or segments, as, for example, in bamboo. Whether the mechanisms governing the establishment of this segmentation pattern in plants are related to that observed in animals is currently unknown. Given the similarity between the patterning of plant and animal body axes, it is possible that the clock and wavefront strategy for generating periodic patterns identified in vertebrates reflects a very general patterning principle for metazoans.

Whether the ultradian oscillator identified in vertebrate segmentation is strictly dedicated to this process or whether it reflects a more fundamental cellular process at work in the embryo remains an open question. Strikingly, *Hes1* oscillations with a period similar to that of somite segmentation in mouse can be recapitulated in cultured cells in response to serum stimulation<sup>68</sup>. Microarray studies of these serum-induced oscillations in mouse C3H10T1/2 fibroblasts and human mesenchymal stem cells identified ultradian oscillations of Smad (MAD homologue) and Stat (signal transducer and activator of transcription) signalling pathways<sup>122,123</sup>. So, the molecular circuitry underlying these oscillations shows some differences from that of the segmentation clock. The key remaining task is the identification of the clock pacemaker that drives the oscillations of cyclic genes in somitogenesis and in these cultured cells. Whereas much has been learned since the identification of the segmentation clock, it currently remains unclear whether the cyclic genes are part of the segmentation clock pacemaker or if they merely reflect an output of a yet-to-be-identified pacemaker.

In humans, severe disruptions of the segmentation pattern of the vertebrae lead to congenital scoliosis, which is a rare deformity of the spine that occurs in 1–2 per 10,000 births<sup>124</sup>. Most forms of congenital scoliosis are thought to be sporadic, but, in fact, little information on familial incidence is available. So far, traditional linkage analysis in families with individuals affected with congenital scoliosis has led to the identification of three genes, all associated with the segmentation clock. Mutations in *Dll3*, *Mesp2* and *Lfng* were shown to lead to familial forms of spondylocostal dysostosis — a form of congenital scoliosis<sup>125–127</sup>. The fact that all of the genes that have been associated with familial

congenital scoliosis so far are linked to the segmentation clock suggests that these anomalies result from defects in the somitogenesis process<sup>124</sup>. In addition, it suggests that the oscillator also operates in human embryos to control segmentation. Studies of the somitogenesis process in mouse embryos point to a number of genes in which mutation results in phenotypes that resemble human congenital scoliosis, providing interesting candidate genes that might carry mutations in the patients. Deciphering the segmentation clock mechanism in model organisms will help improve our knowledge of these diseases, which, in turn, could lead to improved clinical management of these patients.

1. Sadler, T. W. in *Langman's Medical Embryology* (ed. Wilkins, W.A.) (Lippincott Williams & Wilkins, Baltimore, 2000).
2. Richardson, M. K., Allen, S. P., Wright, G. M., Raynaud, A. & Hanken, J. Somite number and vertebrate evolution. *Development* **125**, 151–160 (1998).
3. Couly, G., Coltey, P. & Le Douarin, N. M. The triple origin of skull in higher vertebrates: a study in quail–chick chimeras. *Development* **117**, 409–429 (1993).
4. Kuan, C. Y., Tannahill, D., Cook, G. M. & Keynes, R. J. Somite polarity and segmental patterning of the peripheral nervous system. *Mech. Dev.* **121**, 1055–1068 (2004).
5. Kulesa, P. M. & Fraser, S. E. Cell dynamics during somite boundary formation revealed by time-lapse analysis. *Science* **298**, 991–995 (2002).
6. Hirsinger, E., Jouve, C., Dubrulle, J. & Pourquié, O. Somite formation and patterning. *Int. Rev. Cytol.* **198**, 1–65 (2000).
7. Wellik, D. M. Hox patterning of the vertebrate axial skeleton. *Dev. Dyn.* **236**, 2454–2463 (2007).
8. Kmita, M. & Duboule, D. Organizing axes in time and space; 25 years of colinear tinkering. *Science* **301**, 331–333 (2003).
9. Saga, Y. & Takeda, H. The making of the somite: molecular events in vertebrate segmentation. *Nature Rev. Genet.* **2**, 835–845 (2001).
10. Brent, A. E. & Tabin, C. J. Developmental regulation of somite derivatives: muscle, cartilage and tendon. *Curr. Opin. Genet. Dev.* **12**, 548–557 (2002).
11. Bothe, I., Ahmed, M. U., Winterbottom, F. L., von Scheven, G. & Dietrich, S. Extrinsic versus intrinsic cues in avian paraxial mesoderm patterning and differentiation. *Dev. Dyn.* **236**, 2397–2409 (2007).
12. Nusslein-Volhard, C. & Wieschaus, E. Mutations affecting segment number and polarity in *Drosophila*. *Nature* **287**, 795–801 (1980).
13. Wilkins, A. S. *The Evolution Of Developmental Pathways* (Sinauer Associates, Sunderland, 2001).
14. Cooke, J. & Zeeman, E. C. A clock and wavefront model for control of the number of repeated structures during animal morphogenesis. *J. Theor. Biol.* **58**, 455–476 (1976).  
**The authors propose a theoretical model for somitogenesis postulating the existence of a clock and a wavefront.**
15. Goldbeter, A., Gonze, D. & Pourquié, O. Sharp developmental thresholds defined through bistability by antagonistic gradients of retinoic acid and FGF signaling. *Dev. Dyn.* **236**, 1495–1508 (2007).
16. Dale, J. K. & Pourquié, O. A clock-work somite. *Bioessays* **22**, 72–83 (2000).
17. Kulesa, P. M., Schnell, S., Rudloff, S., Baker, R. E. & Maini, P. K. From segment to somite: Segmentation to epithelialization analyzed within quantitative frameworks. *Dev. Dyn.* **236**, 1392–1402 (2007).
18. Palmeirim, I., Henrique, D., Ish-Horowicz, D. & Pourquié, O. Avian hairy gene expression identifies a molecular clock linked to vertebrate segmentation and somitogenesis. *Cell* **91**, 639–648 (1997).  
**This work provides the first molecular evidence of the existence of a molecular oscillator — called the segmentation clock — linked to somitogenesis, on the basis of the periodic transcriptional expression in the presomitic mesoderm of HES1.**
19. Holley, S. A., Geisler, R. & Nusslein-Volhard, C. Control of her1 expression during zebrafish somitogenesis by a delta-dependent oscillator and an independent wavefront activity. *Genes Dev.* **14**, 1678–1690 (2000).
20. Forsberg, H., Crozet, F. & Brown, N. A. Waves of mouse Lunatic fringe expression, in four-hour cycles at two-hour intervals, precede somite boundary formation. *Curr. Biol.* **8**, 1027–1030 (1998).
21. Jiang, Y. J. *et al.* Notch signalling and the synchronization of the somite segmentation clock. *Nature* **408**, 475–479 (2000).  
**The authors propose a role for Notch signalling in the synchronization between neighbouring cellular oscillators in the PSM.**
22. Li, Y., Fenger, U., Niehrs, C. & Pollet, N. Cyclic expression of *esr9* gene in *Xenopus* presomitic mesoderm. *Differentiation* **71**, 83–89 (2003).
23. Muller, M., v Weizsacker, E. & Campos-Ortega, J. A. Expression domains of a zebrafish homologue of the *Drosophila* pair-rule gene hairy correspond to primordia of alternating somites. *Development* **122**, 2071–2078 (1996).
24. Oates, A. C. & Ho, R. K. Hairy/E(spl)-related (Her) genes are central components of the segmentation oscillator and display redundancy with the Delta/Notch signaling pathway in the formation of anterior segmental boundaries in the zebrafish. *Development* **129**, 2929–2946 (2002).
25. Henry, C. A. *et al.* Two linked hairy/Enhancer of split-related zebrafish genes, *her1* and *her7*, function together to refine alternating somite boundaries. *Development* **129**, 3693–3704 (2002).
26. Gajewski, M., Elmasri, H., Girschick, M., Sieger, D. & Winkler, C. Comparative analysis of her genes during fish somitogenesis suggests a mouse/chick-like mode of oscillation in medaka. *Dev. Genes Evol.* **216**, 315–332 (2006).
27. Shankaran, S. S. *et al.* Completing the set of h/E(spl) cyclic genes in zebrafish: *her12* and *her15* reveal novel modes of expression and contribute to the segmentation clock. *Dev. Biol.* **304**, 615–632 (2007).
28. Sieger, D., Tautz, D. & Gajewski, M. *her11* is involved in the somitogenesis clock in zebrafish. *Dev. Genes Evol.* **214**, 393–406 (2004).
29. van Eeden, F. J. *et al.* Mutations affecting somite formation and patterning in the zebrafish, *Danio rerio*. *Development* **123**, 153–164 (1996).
30. Holley, S. A., Julich, D., Rauch, G. J., Geisler, R. & Nusslein-Volhard, C. *her1* and the Notch pathway function within the oscillator mechanism that regulates zebrafish somitogenesis. *Development* **129**, 1175–1183 (2002).
31. Julich, D. *et al.* *beamter/deltaC* and the role of Notch ligands in the zebrafish somite segmentation, hindbrain neurogenesis and hypochord differentiation. *Dev. Biol.* **286**, 391–404 (2005).
32. Itoh, M. *et al.* Mind bomb is a ubiquitin ligase that is essential for efficient activation of Notch signaling by Delta. *Dev. Cell* **4**, 67–82 (2003).
33. Takke, C. & Campos-Ortega, J. A. *her1*, a zebrafish pair-rule like gene, acts downstream of notch signalling to control somite development. *Development* **126**, 3005–3014 (1999).
34. Gajewski, M. *et al.* Anterior and posterior waves of cyclic *her1* gene expression are differentially regulated in the presomitic mesoderm of zebrafish. *Development* **130**, 4269–4278 (2003).
35. Giudicelli, F., Ozbudak, E. M., Wright, G. J. & Lewis, J. Setting the tempo in development: an investigation of the zebrafish somite clock mechanism. *PLoS Biol.* **5**, e150 (2007).
36. Lewis, J. Autoinhibition with transcriptional delay: a simple mechanism for the zebrafish somitogenesis oscillator. *Curr. Biol.* **13**, 1398–1408 (2003).  
**This paper proposes a mathematical model for the segmentation clock oscillator in zebrafish, based on a negative feedback loop with delay.**
37. Oates, A. C., Mueller, C. & Ho, R. K. Cooperative function of *deltaC* and *her7* in anterior segment formation. *Dev. Biol.* **280**, 133–149 (2005).
38. Riedel-Kruse, I. H., Muller, C. & Oates, A. C. Synchrony dynamics during initiation, failure, and rescue of the segmentation clock. *Science* **317**, 1911–1915 (2007).
39. Davis, R. L. & Turner, D. L. Vertebrate hairy and Enhancer of split related proteins: transcriptional repressors regulating cellular differentiation and embryonic patterning. *Oncogene* **20**, 8342–8357 (2001).
40. Mara, A., Schroeder, J., Chalouni, C. & Holley, S. A. Priming, initiation and synchronization of the segmentation clock by *deltaD* and *deltaC*. *Nature Cell Biol.* **9**, 523–530 (2007).
41. Kawamura, A. *et al.* Zebrafish hairy/enhancer of split protein links FGF signaling to cyclic gene expression in the periodic segmentation of somites. *Genes Dev.* **19**, 1156–1161 (2005).
42. Lewis, J. & Ozbudak, E. M. Deciphering the somite segmentation clock: beyond mutants and morphants. *Dev. Dyn.* **236**, 1410–1415 (2007).
43. Jouve, C. *et al.* Notch signalling is required for cyclic expression of the hairy-like gene *HES1* in the presomitic mesoderm. *Development* **127**, 1421–1429 (2000).
44. Leimeister, C. *et al.* Oscillating expression of *c-hes2* in the presomitic mesoderm suggests that the segmentation clock may use combinatorial signaling through multiple interacting bHLH factors. *Dev. Biol.* **227**, 91–103 (2000).
45. Dunwoodie, S. L. *et al.* Axial skeletal defects caused by mutation in the spondylocostal dysplasia/pudgy gene *Dll3* are associated with disruption of the segmentation clock within the presomitic mesoderm. *Development* **129**, 1795–1806 (2002).
46. Bessho, Y., Miyoshi, G., Sakata, R. & Kageyama, R. *Hes7*: a bHLH-type repressor gene regulated by Notch and expressed in the presomitic mesoderm. *Genes Cells* **6**, 175–185 (2001).
47. Maruhashi, M., Van De Putte, T., Huylebroeck, D., Kondoh, H. & Higashi, Y. Involvement of SIP1 in positioning of somite boundaries in the mouse embryo. *Dev. Dyn.* **234**, 332–338 (2005).
48. McGrew, M. J., Dale, J. K., Fraboulet, S. & Pourquié, O. The lunatic fringe gene is a target of the molecular clock linked to somite segmentation in avian embryos. *Curr. Biol.* **8**, 979–982 (1998).
49. Aulehla, A. & Johnson, R. L. Dynamic expression of lunatic fringe suggests a link between notch signaling and an autonomous cellular oscillator driving somite segmentation. *Dev. Biol.* **207**, 49–61 (1999).
50. Prince, V. E. *et al.* Zebrafish lunatic fringe demarcates segmental boundaries. *Mech. Dev.* **105**, 175–180 (2001).
51. Pourquié, O. Notch around the clock. *Curr. Opin. Genet. Dev.* **9**, 559–565 (1999).
52. Jiang, Y. J., Smithers, L. & Lewis, J. The clock is linked to notch signalling. *Curr. Biol.* **8**, R868–R871 (1998).

53. del Barco Barrantes, I. *et al.* Interaction between Notch signalling and Lunatic Fringe during somite boundary formation in the mouse. *Curr. Biol.* **9**, 470–480 (1999).
54. Huppert, S. S., Ilagan, M. X., De Strooper, B. & Kopan, R. Analysis of Notch function in presomitic mesoderm suggests a gamma-secretase-independent role for presenilins in somite differentiation. *Dev. Cell* **8**, 677–688 (2005).
55. Morimoto, M., Takahashi, Y., Endo, M. & Saga, Y. The Mesp2 transcription factor establishes segmental borders by suppressing Notch activity. *Nature* **435**, 354–359 (2005).
- The authors characterize the role of Mesp2 in defining the segment boundary.**
56. Dale, J. K. *et al.* Periodic Notch inhibition by Lunatic Fringe underlies the chick segmentation clock. *Nature* **421**, 275–278 (2003).
57. Serth, K., Schuster-Gossler, K., Cordes, R. & Gossler, A. Transcriptional oscillation of Lunatic fringe is essential for somitogenesis. *Genes Dev.* **17**, 912–925 (2003).
58. Bessho, Y., Hirata, H., Masamizu, Y. & Kageyama, R. Periodic repression by the bHLH factor Hes7 is an essential mechanism for the somite segmentation clock. *Genes Dev.* **17**, 1451–1456 (2003).
59. Ishibashi, M. *et al.* Targeted disruption of mammalian hairy and Enhancer of split homolog-1 (HES-1) leads to up-regulation of neural helix-loop-helix factors, premature neurogenesis, and severe neural tube defects. *Genes Dev.* **9**, 3136–3148 (1995).
60. Ohtsuka, T. *et al.* Hes1 and Hes5 as notch effectors in mammalian neuronal differentiation. *EMBO J.* **18**, 2196–2207 (1999).
61. Kokubo, H., Miyagawa-Tomita, S., Nakazawa, M., Saga, Y. & Johnson, R. L. Mouse hesr1 and hesr2 genes are redundantly required to mediate Notch signaling in the developing cardiovascular system. *Dev. Biol.* **278**, 301–309 (2005).
62. Bessho, Y. *et al.* Dynamic expression and essential functions of Hes7 in somite segmentation. *Genes Dev.* **15**, 2642–2647 (2001).
63. Morales, A. V., Yasuda, Y. & Ish-Horowitz, D. Periodic lunatic fringe expression is controlled during segmentation by a cyclic transcriptional enhancer responsive to Notch signaling. *Dev. Cell* **5**, 63–74 (2002).
64. Cole, S. E., LeVorse, J. M., Tilghman, S. M. & Vogt, T. F. Clock regulatory elements control cyclic expression of lunatic fringe during somitogenesis. *Dev. Cell* **3**, 75–84 (2002).
65. Shifley, E. T. *et al.* Oscillatory lunatic fringe activity is crucial for segmentation of the anterior but not posterior skeleton. *Development* **135**, 899–908 (2008).
66. Hirata, H. *et al.* Instability of Hes7 protein is crucial for the somite segmentation clock. *Nature Genet.* **36**, 750–754 (2004).
67. Monk, N. A. M. Oscillatory expression of Hes1, p53 and NF- $\kappa$ B driven by transcriptional time delays. *Curr. Biol.* **13**, 1409–1413 (2003).
68. Hirata, H. *et al.* Oscillatory expression of the bHLH factor Hes1 regulated by a negative feedback loop. *Science* **298**, 840–843 (2002).
- This work shows that Hes1 oscillations are induced by serum stimulation in mouse fibroblasts, with a period similar to the mouse segmentation clock.**
69. Aulehla, A. *et al.* Wnt3a plays a major role in the segmentation clock controlling somitogenesis. *Dev. Cell* **4**, 395–406 (2003).
- The authors first report the implication of Wnt signalling in the mouse segmentation clock.**
70. Dequeant, M. L. *et al.* A complex oscillating network of signaling genes underlies the mouse segmentation clock. *Science* **314**, 1595–1598 (2006).
- This work provides the first systematic approach of the segmentation clock regulatory network uncovering the existence of a large number of cyclic genes participating in negative feedback loops linked to the Notch, Wnt and FGF pathways.**
71. Weidinger, G., Thorpe, C. J., Wuennenberg-Stapleton, K., Ngai, J. & Moon, R. T. The Sp1-related transcription factors sp5 and sp5-like act downstream of Wnt/ $\beta$ -catenin signaling in mesoderm and neuroectoderm patterning. *Curr. Biol.* **15**, 489–500 (2005).
72. He, T. C. *et al.* Identification of c-MYC as a target of the APC pathway. *Science* **281**, 1509–1512 (1998).
73. Glinka, A. *et al.* Dickkopf-1 is a member of a new family of secreted proteins and functions in head induction. *Nature* **391**, 357–362 (1998).
74. Yu, H. M. *et al.* The role of Axin2 in calvarial morphogenesis and craniosynostosis. *Development* **132**, 1995–2005 (2005).
75. MacDonald, B. T., Adamska, M. & Meisler, M. H. Hypomorphic expression of Dkk1 in the doubleridge mouse: dose dependence and compensatory interactions with Lrp6. *Development* **131**, 2543–2552 (2004).
76. Harrison, S. M., Houzelstein, D., Dunwoodie, S. L. & Beddington, R. S. Sp5, a new member of the Sp1 family, is dynamically expressed during development and genetically interacts with Brachyury. *Dev. Biol.* **227**, 358–372. (2000).
77. Trumpp, A. *et al.* c-Myc regulates mammalian body size by controlling cell number but not cell size. *Nature* **414**, 768–773 (2001).
78. Camenisch, T. D. *et al.* Disruption of hyaluronan synthase-2 abrogates normal cardiac morphogenesis and hyaluronan-mediated transformation of epithelium to mesenchyme. *J. Clin. Invest.* **106**, 349–360 (2000).
79. Dunty, W. C., Jr. *et al.* Wnt3a/ $\beta$ -catenin signaling controls posterior body development by coordinating mesoderm formation and segmentation. *Development* **135**, 85–94 (2008).
80. Aulehla, A. *et al.* A  $\beta$ -catenin gradient links the clock and wavefront systems in mouse embryo segmentation. *Nature Cell Biol.* **10**, 186–193 (2008).
81. Lamar, E. *et al.* Nrarp is a novel intracellular pathway component of the Notch signaling pathway. *Genes Dev.* **15**, 1885–1899 (2001).
82. Krebs, L. T., Defetos, M. L., Bevan, M. J. & Gridley, T. The Nrarp gene encodes an ankyrin-repeat protein that is transcriptionally regulated by the notch signaling pathway. *Dev. Biol.* **238**, 110–119 (2001).
83. Pirot, P., van Grunsven, L. A., Marine, J. C., Huylebroeck, D. & Bellefroid, E. J. Direct regulation of the Nrarp gene promoter by the Notch signaling pathway. *Biochem. Biophys. Res. Commun.* **322**, 526–534 (2004).
84. Ishitani, T., Matsumoto, K., Chitnis, A. B. & Itoh, M. Nrarp functions to modulate neural-crest-cell differentiation by regulating LEF1 protein stability. *Nature Cell Biol.* **7**, 1106–1112 (2005).
85. Ishikawa, A. *et al.* Mouse Nkd1, a Wnt antagonist, exhibits oscillatory gene expression in the PSM under the control of Notch signaling. *Mech. Dev.* **121**, 1443–1453 (2004).
86. Dale, J. K. *et al.* Oscillations of the snail genes in the presomitic mesoderm coordinate segmental patterning and morphogenesis in vertebrate somitogenesis. *Dev. Cell* **10**, 355–366 (2006).
87. Niwa, Y. *et al.* The initiation and propagation of Hes7 oscillation are cooperatively regulated by Fgf and notch signaling in the somite segmentation clock. *Dev. Cell* **13**, 298–304 (2007).
88. Wahl, M. B., Deng, C., Lewandoski, M. & Pourquié, O. FGF signaling acts upstream of the NOTCH and WNT signaling pathways to control segmentation clock oscillations in mouse somitogenesis. *Development* **134**, 4033–4041 (2007).
89. Aulehla, A. & Herrmann, B. G. Segmentation in vertebrates: clock and gradient finally joined. *Genes Dev.* **18**, 2060–2067 (2004).
90. Nakaya, M. A. *et al.* Wnt3a links left-right determination with segmentation and anteroposterior axis elongation. *Development* **132**, 5425–5436 (2005).
91. Elsdale, T., Pearson, M. & Whitehead, M. Abnormalities in somite segmentation following heat shock to Xenopus embryos. *J. Embryol. Exp. Morphol.* **35**, 625–635 (1976).
92. Dubrulle, J., McGrew, M. J. & Pourquié, O. FGF signaling controls somite boundary position and regulates segmentation clock control of spatiotemporal Hox gene activation. *Cell Biol.* **106**, 219–232 (2001).
- This work reports the first evidence of the role of FGF signalling as a key component of the wavefront in the chicken embryo.**
93. Delfini, M. C., Dubrulle, J., Malapert, P., Chal, J. & Pourquié, O. Control of the segmentation process by graded MAPK/ERK activation in the chick embryo. *Proc. Natl Acad. Sci. USA* **102**, 11343–11348 (2005).
94. Linask, K. K. *et al.* N-cadherin/catenin-mediated morphoregulation of somite formation. *Dev. Biol.* **202**, 85–102 (1998).
95. Duband, J. L. *et al.* Adhesion molecules during somitogenesis in the avian embryo. *J. Cell Biol.* **104**, 1361–1374 (1987).
96. Horikawa, K. R. G., Takeichi M., Chisaka O. Adhesive subdivisions intrinsic to the epithelial somites. *Dev. Biol.* **215**, 182–189 (1999).
97. Burgess, R., Cserjesi, P., Ligon, K. L. & Olson, E. N. Paraxis: a basic helix-loop-helix protein expressed in paraxial mesoderm and developing somites. *Dev. Biol.* **168**, 296–306 (1995).
98. Nakaya, Y., Kuroda, S., Katagiri, Y. T., Kaibuchi, K. & Takahashi, Y. Mesenchymal–epithelial transition during somitic segmentation is regulated by differential roles of Cdc42 and Rac1. *Dev. Cell* **7**, 425–438 (2004).
99. Sawada, A. *et al.* Fgf/MAPK signalling is a crucial positional cue in somite boundary formation. *Development* **128**, 4873–4880 (2001).
100. Dubrulle, J. & Pourquié, O. fgf8 mRNA decay establishes a gradient that couples axial elongation to patterning in the vertebrate embryo. *Nature* **427**, 419–422 (2004).
101. Reifers, F. *et al.* Fgf8 is mutated in zebrafish acerebellar (ace) mutants and is required for maintenance of midbrain-hindbrain boundary development and somitogenesis. *Development* **125**, 2381–2395 (1998).
102. Perantoni, A. O. *et al.* Inactivation of FGF8 in early mesoderm reveals an essential role in kidney development. *Development* **132**, 3859–3871 (2005).
103. Draper, B. W., Stock, D. W. & Kimmel, C. B. Zebrafish fgf24 functions with fgf8 to promote posterior mesodermal development. *Development* **130**, 4639–4654 (2003).
104. Vermot, J. *et al.* Retinoic acid controls the bilateral symmetry of somite formation in the mouse embryo. *Science* **308**, 563–566 (2005).
105. Vermot, J. & Pourquié, O. Retinoic acid coordinates somitogenesis and left-right patterning in vertebrate embryos. *Nature* **435**, 215–220 (2005).
106. Kawakami, Y., Raya, A., Raya, R. M., Rodriguez-Esteban, C. & Belmonte, J. C. Retinoic acid signalling links left-right asymmetric patterning and bilaterally symmetric somitogenesis in the zebrafish embryo. *Nature* **435**, 165–171 (2005).
107. Sirbu, I. O. & Duester, G. Retinoic-acid signalling in node ectoderm and posterior neural plate directs left-right patterning of somitic mesoderm. *Nature Cell Biol.* **8**, 271–277 (2006).
108. Diez del Corral, R. *et al.* Opposing FGF and retinoid pathways control ventral neural pattern, neuronal differentiation, and segmentation during body axis extension. *Neuron* **40**, 65–79 (2003).
109. Moreno, T. A. & Kintner, C. Regulation of segmental patterning by retinoic acid signaling during *Xenopus* somitogenesis. *Dev. Cell* **6**, 205–218 (2004).
110. Niederreither, K., Fraulob, V., Garnier, J. M., Chambon, P. & Dolle, P. Differential expression of retinoic acid-synthesizing (RALDH) enzymes during fetal development and organ differentiation in the mouse. *Mech. Dev.* **110**, 165–171 (2002).
111. Abu-Abed, S. *et al.* The retinoic acid-metabolizing enzyme, CYP26A1, is essential for normal hindbrain patterning, vertebral identity, and development of posterior structures. *Genes Dev.* **15**, 226–240 (2001).
112. Niederreither, K. *et al.* Genetic evidence that oxidative derivatives of retinoic acid are not involved in retinoid signaling during mouse development. *Nature Genet.* **31**, 84–88 (2002).
113. Dubrulle, J. & Pourquié, O. Coupling segmentation to axis formation. *Development* **131**, 5783–5793 (2004).
114. Takahashi, Y. *et al.* Mesp2 initiates somite segmentation through the Notch signalling pathway. *Nature Genet.* **25**, 390–396 (2000).
115. Morimoto, M. *et al.* The negative regulation of Mesp2 by mouse Ripply2 is required to establish the rostro-caudal patterning within a somite. *Development* **134**, 1561–1569 (2007).
116. Kawamura, A. *et al.* Groucho-associated transcriptional repressor ripply1 is required for proper transition from the presomitic mesoderm to somites. *Dev. Cell* **9**, 735–744 (2005).
117. Nakajima, Y., Morimoto, M., Takahashi, Y., Koseki, H. & Saga, Y. Identification of Epha4 enhancer required for segmental expression and the regulation by Mesp2. *Development* **133**, 2517–2525 (2006).
118. Francois, P., Hakim, V. & Siggia, E. D. Deriving structure from evolution: metazoan segmentation. *Mol. Syst. Biol.* **3**, 154 (2007).
119. Davis, G. K. & Patel, N. H. The origin and evolution of segmentation. *Trends Cell Biol.* **9**, 68–72 (1999).
120. Stollewerk, A., Schoppmeier, M. & Damen, W. G. Involvement of Notch and Delta genes in spider segmentation. *Nature* **423**, 863–865 (2003).
121. Dunlap, J. C. & Loros, J. J. The neurospora circadian system. *J. Biol. Rhythms* **19**, 414–424 (2004).
122. Yoshiura, S. *et al.* Ultradian oscillations of Stat., Smad, and Hes1 expression in response to serum. *Proc. Natl Acad. Sci. USA* **104**, 11292–11297 (2007).

123. William, D. A. *et al.* Identification of oscillatory genes in somitogenesis from functional genomic analysis of a human mesenchymal stem cell model. *Dev. Biol.* **305**, 172–186 (2007).
124. Turnpenny, P. D. *et al.* Abnormal vertebral segmentation and the notch signaling pathway in man. *Dev. Dyn.* **236**, 1456–1474 (2007).
125. Bulman, M. P. *et al.* Mutations in the human delta homologue, DLL3, cause axial skeletal defects in spondylocostal dysostosis. *Nature Genet.* **24**, 438–441 (2000).
126. Whittock, N. V. *et al.* Mutated MESP2 causes spondylocostal dysostosis in humans. *Am. J. Hum. Genet.* **74**, 1249–1254 (2004).
127. Sparrow, D. B. *et al.* Mutation of the LUNATIC FRINGE gene in humans causes spondylocostal dysostosis with a severe vertebral phenotype. *Am. J. Hum. Genet.* **78**, 28–37 (2006).
128. Horikawa, K., Ishimatsu, K., Yoshimoto, E., Kondo, S. & Takeda, H. Noise-resistant and synchronized oscillation of the segmentation clock. *Nature* **441**, 719–723 (2006).  
**This work provides experimental evidence supporting the role of Notch in the synchronization between neighbouring PSM cells oscillations.**
129. Ishimatsu, K., Horikawa, K. & Takeda, H. Coupling cellular oscillators: a mechanism that maintains synchrony against developmental noise in the segmentation clock. *Dev. Dyn.* **236**, 1416–1421 (2007).
130. Maroto, M., Dale, J. K., Dequeant, M. L., Petit, A. C. & Pourquié, O. Synchronised cycling gene oscillations in presomitic mesoderm cells require cell-cell contact. *Int. J. Dev. Biol.* **49**, 309–315 (2005).
131. Masamizu, Y. *et al.* Real-time imaging of the somite segmentation clock: revelation of unstable oscillators in the individual presomitic mesoderm cells. *Proc. Natl Acad. Sci. USA* **103**, 1313–1318 (2006).  
**This work provides the first real-time imaging of the segmentation clock oscillations in mouse presomitic mesoderm using a luciferase-based reporter fused to the *Hes1* promoter.**
132. Pourquié, O. & Tam, P. P. A nomenclature for prospective somites and phases of cyclic gene expression in the presomitic mesoderm. *Dev. Cell* **1**, 619–620 (2001).
133. Ordahl, C. P. in *Molecular Basis of Morphogenesis* (ed. Bernfield, M.) pp 165–176 (John Wiley and Sons, New York, 1993).

## Acknowledgements

The authors thank A. Aulehla and to E. Ozbudak for critical reading of the manuscript. Work in the Pourquié laboratory is supported by NIH grant R02HD043,158 to O.P. and by Stowers Institute for Medical Research. O.P. is a Howard Hughes Medical Institute Investigator.

## DATABASES

Entrez Gene: <http://www.ncbi.nlm.nih.gov/entrez/query.fcgi?db=gene>  
[Axin2](#) | [bicoid](#) | [Brachyury](#) | [Dll1](#) | [Dusp4](#) | [Dusp6](#) | [engrailed](#) | [Epha4](#) | [even-skipped](#) | [Egfr3](#) | [Egfr4](#) | [Egfr8](#) | [Egfr18](#) | [fgf24](#) | [Fgfr1](#) | [hair1](#) | [has2](#) | [hedgehog](#) | [her1](#) | [her2](#) | [her11](#) | [her12](#) | [her15](#) | [Hes5](#) | [Hey1](#) | [HEY2](#) | [hunchback](#) | [Kruppel](#) | [Lfng](#) | [Mesp2](#) | [Msn1](#) | [Myod](#) | [nanos](#) | [Nkd1](#) | [Nrarp](#) | [Rbpjk](#) | [runt](#) | [Snai1](#) | [SNAIL2](#) | [Spry2](#) | [wingless](#) | [Wnt3a](#)  
 UniProtKB: <http://ca.expasy.org/sprot>  
 β-catenin | [CDC42](#) | [CYP26](#) | [DACT1](#) | [DeltaC](#) | [DeltaD](#) | [DKK1](#) | [ERK](#) | [LEF1](#) | [Mindbomb](#) | [MYC](#) | [Nodal](#) | [Notch1A](#) | [RAC1](#) | [RALDH2](#) | [Ripply1](#) | [SP5](#) | [TCF15](#)

## FURTHER INFORMATION

Olivier Pourquié's homepage:  
<http://research.stowers-institute.org/pourquielab/>

ALL LINKS ARE ACTIVE IN THE ONLINE PDF